

K^-N interaction in nuclear medium and kaonic atoms

Jaroslava Óbertová

*Faculty of Nuclear Sciences and Physical Engineering,
Czech Technical University in Prague*

in collaboration with

Àngels Ramos

University of Barcelona

Eliahu Friedman

Hebrew University, Jerusalem

Jiří Mareš

NPI, Řež

KAMPAL workshop, 30 September - 4 October 2024, Trento, Italy

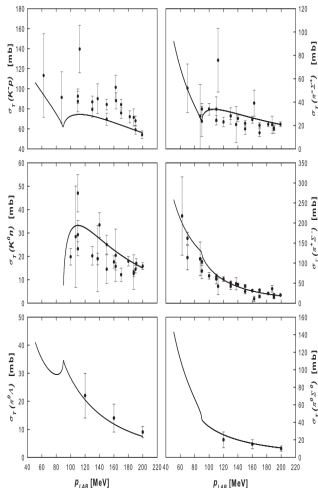
In memory of Johann Zmeskal



LEAP2016, Kanazawa, Japan

K^-N interactions

K^-p scattering:



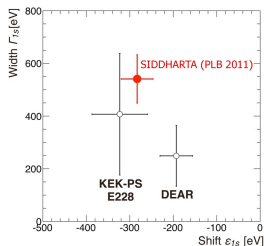
Threshold branching ratios:

$$\gamma = \frac{\Gamma(K^-p \rightarrow \pi^+\Sigma^-)}{\Gamma(K^-p \rightarrow \pi^-\Sigma^+)} = 2.36 \pm 0.04$$

$$R_c = \frac{\Gamma(K^-p \rightarrow \text{charged})}{\Gamma(K^-p \rightarrow \text{all})} = 0.664 \pm 0.011$$

$$R_n = \frac{\Gamma(K^-p \rightarrow \pi^0\Lambda)}{\Gamma(K^-p \rightarrow \text{neutral})} = 0.189 \pm 0.015$$

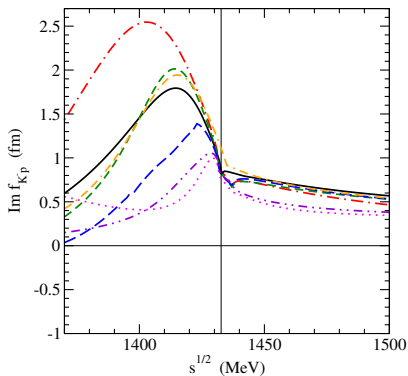
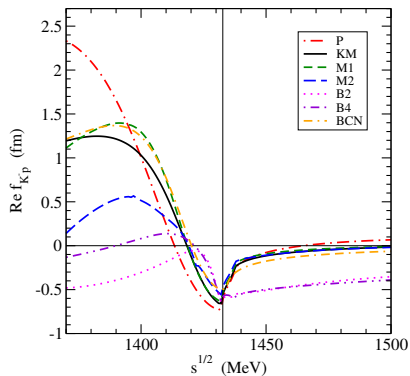
Kaonic hydrogen:



- K^-p data well described by several chiral models

A. Cieplý, M. Mai, U.-G. Meissner, J. Smejkal, NPA 945 (2016) 17

Free-space K^-p amplitudes in various chiral models



Prague (P)

Kyoto-Munich (KM)

Murcia (M1 and M2)

Bonn (B2 and B4)

Barcelona (BCN)

A. Cieply, J. Smejkal, *Nucl. Phys. A* 881 (2012) 115

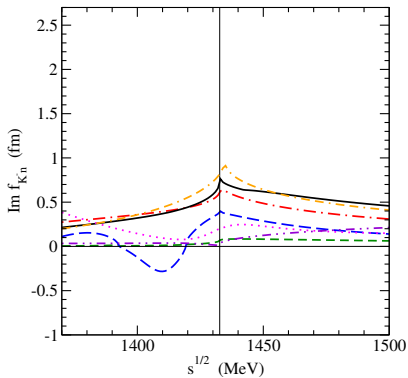
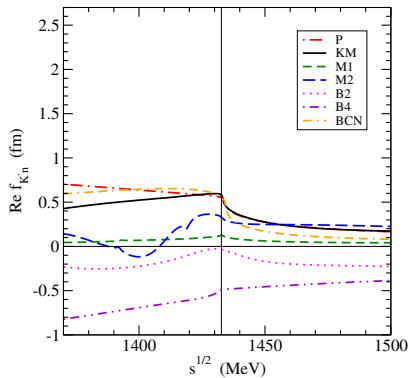
Y. Ikeda, T. Hyodo, W. Weise, *Nucl. Phys. A* 881 (2012) 98

Z. H. Guo, J. A. Oller, *Phys. Rev. C* 87 (2013) 035202

M. Mai, U.-G. Meißner, *Nucl. Phys. A* 900 (2013) 51

A. Feijoo, V. Magas, A. Ramos, *Phys. Rev. C* 99 (2019) 035211

Free-space K^-n amplitudes



Kaonic atoms

- Info about K^-N interaction below threshold provided by kaonic atoms
65 data points (energy shifts, widths, yields=upper level widths)
from CERN, Argonne, RAL, BNL
- Chirally motivated models fail to describe kaonic atom data
E. Friedman, A. Gal, NPA 959 (2017) 66

model	B2	B4	M1	M2	P	KM
$\chi^2(65)$	1174	2358	2544	3548	2300	1806

Multinucleon processes

- Chiral models include only $K^- N \rightarrow \pi Y$ ($Y = \Lambda, \Sigma$) decay channel
- K^- interactions with two and more nucleons should be included, (e.g., $K^- + N + N \rightarrow Y + N$) ← analysis of kaonic atom data

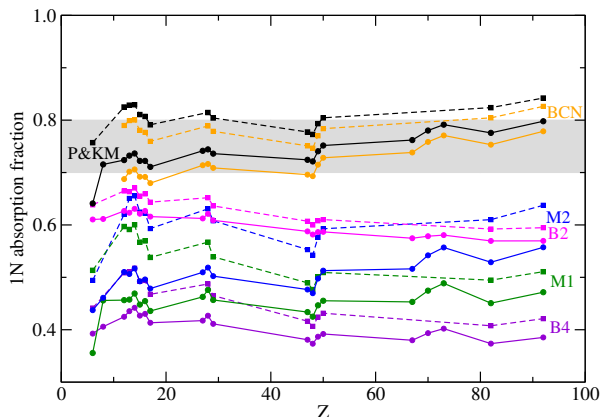
E. Friedman, A. Gal, NPA 959 (2017) 66

$$V_{K^- \text{-multi}N}^{\text{phen}} = -4\pi B \left(\frac{\rho}{\rho_0} \right)^\alpha \rho$$

B is a complex amplitude, ρ is nuclear density distribution, ρ_0 is saturation density and α is positive

- equally good description of data with $\chi^2/\text{dof} \leq 2$

Single- vs. multi-nucleon processes



- Fraction of *single-nucleon* absorption 0.75 ± 0.05 (average value) used as an **additional constraint**.

→ Only **P**, **KM** and **BCN** models found acceptable in kaonic atom analysis

E. Friedman, A. Gal, NPA 959 (2017) 66

Multinucleon processes

- K^- multi-nucleon absorption in the surface region of atomic nuclei represents about 20%
NC 53 (1968) 313 (Berkeley), NPB 35 (1971) 332 (BNL), NC 39A (1977) 538 (CERN)
- K^- multi-nucleon absorption in atoms described by phenomenological optical potential
E. Friedman, A. Gal, NPA 959 (2017) 66
- Model for $K^- NN$ absorption in nuclear matter using free-space chiral amplitudes
T. Sekihara et al., PRC 86 (2012) 065205
- New experimental data on $K^- NN$ absorption (AMADEUS@DAΦNE)
K. Piscicchia et al., PLB 782 (2018) 339
R. Del Grande et al., EPJ C79 (2019) 190
- Solid microscopic model for $K^- NN$ absorption needed!

Microscopic model for $K^- NN$ absorption in nuclear matter

Microscopic model for K^- two-nucleon absorption in symmetric nuclear matter *J. Hrtánková, Á. Ramos, PRC 101 (2020) 035204*

- based on a meson-exchange approach
H. Nagahiro et al., PLB 709 (2012) 87
- **P** and **BCN** chiral $K^- N$ amplitudes employed
- **Pauli correlations** in the medium for $K^- N$ amplitudes considered
- **real part of the $K^- NN$ optical potential** evaluated as well
- $K^- N$ optical potential derived within the same approach

K^-N absorption in nuclear matter

$$K^-N \rightarrow \pi Y \quad (Y = \Lambda, \Sigma)$$

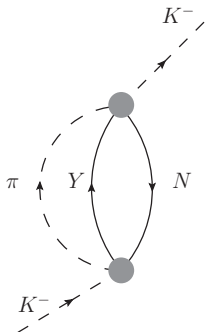


Fig.1: Feynman diagram for K^- absorption on a single nucleon in nuclear matter. The shaded circles denote the K^-N t-matrices derived from a chiral model.

$K^- NN$ absorption in nuclear matter

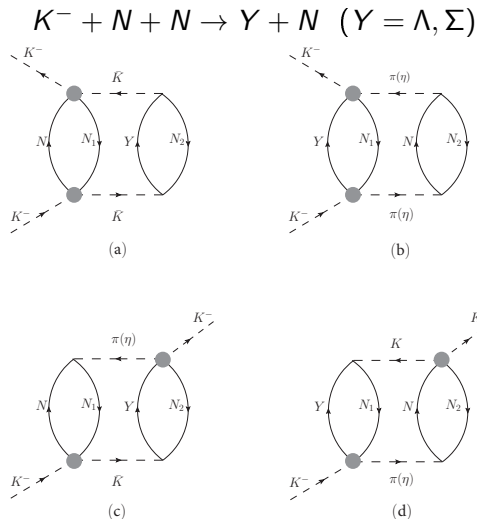


Fig.2: Two-fermion-loop (2FL) Feynman diagrams for non-mesonic K^- absorption on two nucleons N_1, N_2 in nuclear matter. The shaded circles denote the $K^- N$ t-matrices derived from a chiral model.

K^-NN absorption in nuclear matter

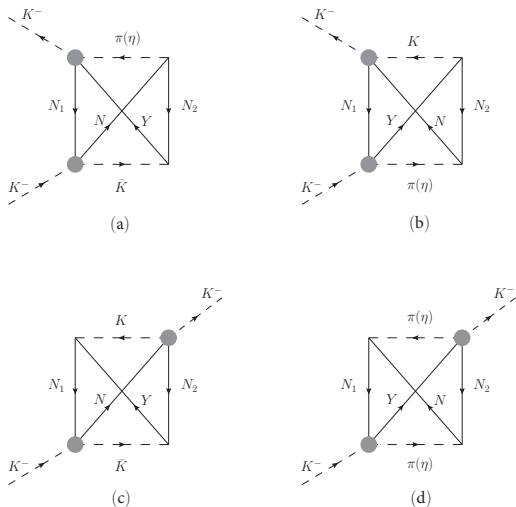


Fig.3: One-fermion-loop (1FL) Feynman diagrams for non-mesonic K^- absorption on two nucleons N_1 , N_2 in nuclear matter. The shaded circles denote the K^-N t-matrices derived from a chiral model.

$K^- NN$ absorption in nuclear matter

$$V_{K^- N} = \sum_{\text{channels}} V_{K^- N \rightarrow \pi Y} \text{ (Fig.1)}$$

$$V_{K^- NN} = \sum_{\text{channels}} V_{K^- NN}^{2\text{FL}} + V_{K^- NN}^{1\text{FL}} \text{ (Fig.2 and 3)}$$

→ contributions from 37 2FL and 28+33 1FL diagrams

Table 1: All considered channels for mesonic and non-mesonic K^- absorption in matter.

$K^- N$	$\rightarrow \pi Y$	$K^- N_1 N_2$	$\rightarrow YN$
$K^- p$	$\rightarrow \pi^0 \Lambda$	$K^- pp$	$\rightarrow \Lambda p$
	$\rightarrow \pi^0 \Sigma^0$		$\rightarrow \Sigma^0 p$
	$\rightarrow \pi^+ \Sigma^-$		$\rightarrow \Sigma^+ n$
	$\rightarrow \pi^- \Sigma^+$	$K^- pn(np)$	$\rightarrow \Lambda n$
$K^- n$	$\rightarrow \pi^- \Lambda$		$\rightarrow \Sigma^0 n$
	$\rightarrow \pi^- \Sigma^0$		$\rightarrow \Sigma^- p$
	$\rightarrow \pi^0 \Sigma^-$	$K^- nn$	$\rightarrow \Sigma^- n$

AMADEUS: Ratio for 2N absorption

Recently measured ratio *R. Del Grande et al., EPJ C79 (2019) 190*

$$R = \frac{\text{BR}(K^- pp \rightarrow \Lambda p)}{\text{BR}(K^- pp \rightarrow \Sigma^0 p)} = 0.7 \pm 0.2(\text{stat.})_{-0.3}^{+0.2}(\text{syst.})$$

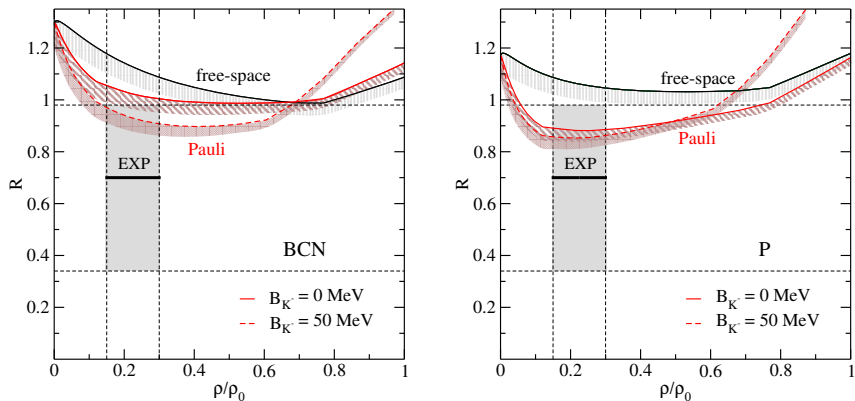


Fig.4: The ratio R as a function of relative density, calculated using the free-space and Pauli blocked amplitudes for $B_{K^-} = 0$ MeV and $B_{K^-} = 50$ MeV. Color bands denote the uncertainty due to different cut-off values $\Lambda_c = 800 - 1200$ MeV.

Branching ratios for mesonic and non-mesonic absorption

Table 2: Primary-interaction ratios (in %) for mesonic absorption of K^- in nuclear matter, calculated with free-space and Pauli blocked BCN amplitudes for $B_{K^-} = 0$ MeV and $p_{K^-} = 0$ MeV/c. The errors denote the uncertainty due to the cut-off dependence. The experimental data corrected for primary interaction are shown for comparison.

BCN mesonic ratio	$0.3\rho_0$		Exp.	
	f.s.	Pauli	${}^4\text{He}$ [1]	${}^{12}\text{C}$ [1]
$\Sigma^+\pi^-/K^-$	19.6 ± 0.6	28.8 ± 0.7	31.2 ± 5.0	29.4 ± 1.0
$\Sigma^-\pi^0/K^-$	6.2 ± 0.2	5.7 ± 0.1	4.9 ± 1.3	2.6 ± 0.6
$\Sigma^-\pi^+/K^-$	21.9 ± 0.6	14.8 ± 0.4	9.1 ± 1.6	13.1 ± 0.4
$\Sigma^0\pi^-/K^-$	6.2 ± 0.2	5.7 ± 0.1	4.9 ± 1.3	2.6 ± 0.6
$\Sigma^0\pi^0/K^-$	18.1 ± 0.5	19.2 ± 0.5	17.7 ± 2.9	20.0 ± 0.7
$\Lambda\pi^0/K^-$	3.8 ± 0.1	3.5 ± 0.1	5.2 ± 1.6	3.4 ± 0.2
$\Lambda\pi^-/K^-$	7.6 ± 0.2	7.0 ± 0.2	10.5 ± 3.0	6.8 ± 0.3
total 1N ratio	83.3 ± 2.4	84.6 ± 2.2	83.5 ± 7.1	77.9 ± 1.6
total 2N ratio	16.7 ± 2.4	15.4 ± 2.2	16.4 ± 2.6	$16 \pm 3(\text{stat.})_{-5}^{+4}(\text{syst.})$ [2]

[1] *C. Vander Velde-Wilquet et al., NC 39 A (1977) 538*

[2] *R. Del Grande et al., EPJ. C 79 (2019) 190*

Model improvement - hadron self-energies

- inclusion of Y , N , K^- and π self-energies into the K^-N chiral BCN amplitudes as well as into the K^-NN model.
- considered baryon potentials

$$V_N = -70 \frac{\rho}{\rho_0} ,$$

$$V_\Lambda = -340\rho + 1087.5\rho^2 \rightarrow V_\Lambda(\rho_0) = -26.4 \text{ MeV},$$

$$V_\Sigma = 30 \frac{\rho}{\rho_0} .$$

- considered pion S- and P-wave self-energy

A. Ramos, E. Oset, NPA 671 (2000) 481

Hadron self-energies: K^-p amplitudes

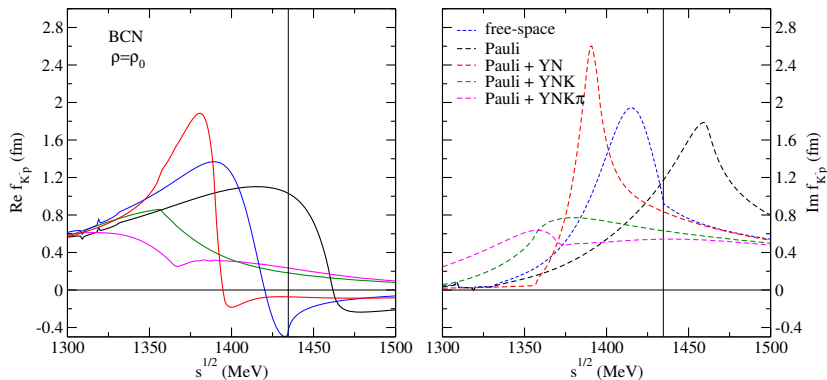


Fig.5: Comparison of $K^-p \rightarrow K^-p$ BCN amplitudes with Pauli blocking only (black), Pauli+YN SE (red), Pauli + YNK^- SE (green), and Pauli + $YNK^- \pi$ SE (magenta) at saturation density $\rho_0 = 0.17 \text{ fm}^{-3}$.

Hadron self-energies: K^-n amplitudes

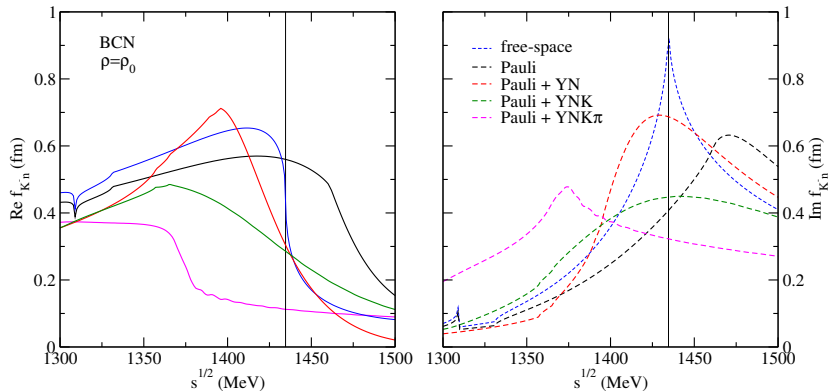


Fig.6: Comparison of $K^-n \rightarrow K^-n$ BCN amplitudes with Pauli blocking only (black), Pauli+YN SE (red), Pauli + YNK $^-$ SE (green), and Pauli + YNK $^-$ π SE (magenta) at saturation density $\rho_0 = 0.17 \text{ fm}^{-3}$.

Comparison with AMADEUS measurement

K. Piscicchia et al., PLB 782 (2018)339

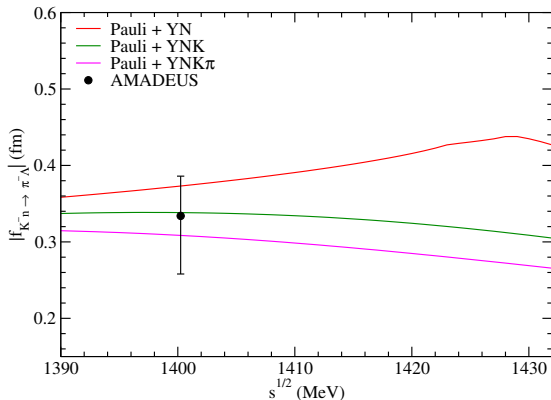


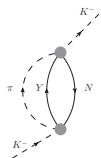
Fig.7: Comparison of $|f_{K^- n \rightarrow \pi^- \Lambda}|$ measured by AMADEUS with in-medium amplitudes: Pauli + YN SE (red), Pauli+YNK SE (green), and Pauli + YNK π SE (magenta) from the BCN model (taken at $\rho = 0.3\rho_0$).

Hadron self-energies: K^- potential

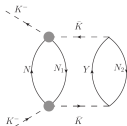
- Pauli + YN SE amplitudes $\Rightarrow V_{K^-} = V_{K^-N} + V_{K^-NN}$
- Pauli + YNK^- ($YNK^-\pi$) SE amplitudes



$$V_{K^-} = t\rho + V_{K^-NN}^{\text{corr}}$$

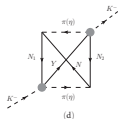
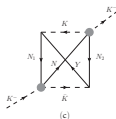
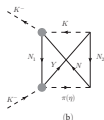
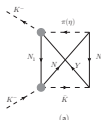


+



+

... +



Hadron self-energies: total K^- potential

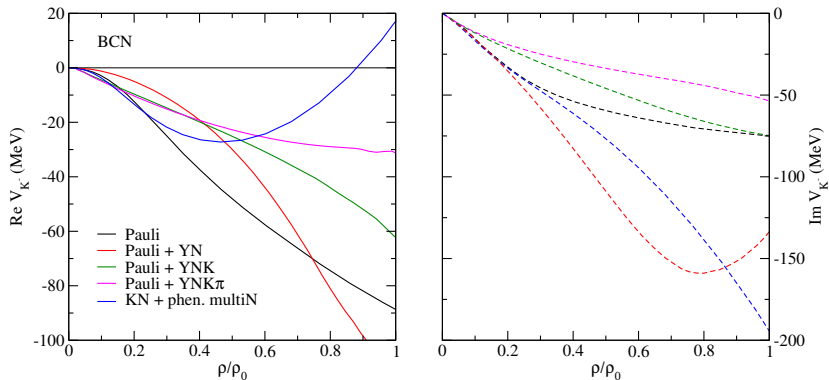


Fig.8: Real (left) and imaginary (right) parts of the total K^- potential as a function of relative density ρ/ρ_0 , calculated with Pauli (black), Pauli + YN SE (red), Pauli + YNK $^-$ SE (green), and Pauli + YNK $^-$ π SE (magenta) BCN amplitudes. For comparison there is the best fit K^-N + phen. multiN potential (blue) based on BCN amplitudes.

Calculations of kaonic atoms

Table 3: Values of $\chi^2(65)$ obtained in calculations of kaonic atoms (24 nuclear species, 65 data points) using $K^-N + K^-NN$ potentials based on BCN Pauli, Pauli+YN, Pauli+YNK, and Pauli+YNK π amplitudes. For comparison, there are also results of calculations with K^-N +phen. multiN potential based on WRW modified BCN amplitudes (*T. Wass, M. Rho, W. Weise, NPA 617 (1997) 449*).

BCN	Pauli	Pauli+YN	Pauli+YNK	Pauli+YNK π	WRW
	$K^-N + K^-NN$	$K^-N + K^-NN$	$t\rho + V_{K^-NN}^{corr}$	$t\rho + V_{K^-NN}^{corr}$	$K^-N + \text{phen. multiN}$
$\chi^2(65)$	553.2	265.5	162.2	93.2	110.7
χ^2/dof	8.5	4.1	2.5	1.4	1.7

- A. Baca et al., NPA 673 (2000), obtained value of $\chi^2/\text{dof} = 3.8$ with K^- potential based on chiral model of Oset and Ramos, NPA 671 (2000).

Calculated branching ratios in $^{12}\text{C}+K^-$ atom

Table 4: Primary-interaction branching ratios (in %) for mesonic ($K^-N \rightarrow Y\pi$, $Y = \Lambda, \Sigma$) and non-mesonic absorption ($K^-NN \rightarrow YN$) of K^- in $^{12}\text{C}+K^-$ atom (3d level), calculated with total K^- potentials based on Pauli + YNK π BCN amplitudes. The K^-N potential was calculated with Pauli+YNK π and WRW modified BCN amplitudes. The experimental data corrected for primary interaction are shown for comparison.

PRELIMINARY RESULT

$^{12}\text{C} + K^-$ (3d) mesonic ratio	BCN		Exp.	
	Pauli+YNK π	WRW	[1]	[2]
$\Sigma^+\pi^-$	14.4	24.0	29.4 ± 1.0	14.4 ± 2.3
$\Sigma^-\pi^0$	8.1	7.7	2.6 ± 0.6	1.2 ± 0.4
$\Sigma^-\pi^+$	12.8	15.8	13.1 ± 0.4	10.3 ± 1.7
$\Sigma^0\pi^-$	8.2	7.8	2.6 ± 0.6	1.2 ± 0.4
$\Sigma^0\pi^0$	10.0	16.3	20.0 ± 0.7	11.8 ± 1.4
$\Lambda\pi^0$	5.3	5.3	3.4 ± 0.2	11.8 ± 1.0
$\Lambda\pi^-$	11.1	10.4	6.8 ± 0.3	23.6 ± 1.9
total 1N ratio	70.0	87.3	77.9 ± 1.6	74.3 ± 3.9
total multiN ratio	30.0	12.7	19.0 ± 2.0	25.7 ± 3.1
			$21 \pm 3(\text{stat.})$	$_{-6}^{+5}(\text{sys.})$ [3]

[1] C. Vander Velde-Wilquet et al., *NC 39 A* (1977) 538

[2] H. Davis et al., *NC 53 A* (1968) 313

[3] R. Del Grande et al., *EPJ C79* (2019) 190

Calculated branching ratios in $^{20}\text{Ne}+K^-$ atom

Table 5: Primary-interaction branching ratios (in %) for mesonic ($K^-N \rightarrow Y\pi$, $Y = \Lambda, \Sigma$) and non-mesonic absorption ($K^-NN \rightarrow YN$) of K^- in $^{20}\text{Ne}+K^-$ atom (3d level), calculated with total potential based on Pauli + YNK π BCN amplitudes. The K^-N potential was calculated with Pauli+YNK π amplitudes and with WRW modified K^-N amplitudes. The experimental data corrected for primary interaction are shown for comparison.

PRELIMINARY RESULT

$^{20}\text{Ne} + K^-$ (3d) mesonic ratio	BCN		Exp. [4]
	Pauli+YNK π	WRW	
$\Sigma^+\pi^-$	14.0	23.5	29.2 ± 2.9
$\Sigma^-\pi^0$	7.0	6.9	1.6 ± 0.7
$\Sigma^-\pi^+$	10.8	14.0	15.8 ± 2.4
$\Sigma^0\pi^-$	7.1	6.9	1.6 ± 0.7
$\Sigma^0\pi^0$	9.2	15.3	20.7 ± 1.8
$\Lambda\pi^0$	5.0	5.1	2.6 ± 0.9
$\Lambda\pi^-$	9.9	9.6	5.2 ± 1.3
total 1N ratio	63.0	81.2	76.7 ± 4.6
total multiN ratio	37.0	18.8	22.6 ± 3.0

[4] J.W. Moulder et al., *NPB 35 (1971) 332*

Summary

- K^-N interaction described by chiral meson-baryon coupled channel interaction models
- Interactions of K^- with two and more nucleons important for realistic description of the K^- -nucleus interaction
 - ▶ only P, KM, and BCN models compatible with available data
- We have developed a microscopic model for K^-NN absorption in nuclear matter using amplitudes derived from the P and BCN chiral meson-baryon interaction models

J. Hrtánková, A. Ramos, PRC 101 (2020) 035204

 - ▶ Pauli blocked amplitudes included → medium effects non-negligible
 - ▶ Calculated ratios in a good agreement with experimental data

Summary

- Further improvement of the K^-NN model and K^-N BCN amplitude model \rightarrow inclusion of hadron (Y, N, K^-, π) self-energies
- Considering K^- and π SE $\rightarrow \text{Re}V_{K^-}(\rho_0) \sim -30$ MeV and $\text{Im}V_{K^-}(\rho_0) \sim -50$ MeV
- Calculations of energy shifts and widths in kaonic atoms:
 - ▶ inclusion of K^-NN absorption improves the description of data considerably
J. Óbertová, E. Friedman, J. Mareš, PRC 106 (2022) 065201
 - ▶ **full model Pauli+YNK π SE describes the data as good as the best fit K^-N +phen. multiN potential based on BCN amplitudes!**

BACK UP

Back up slides

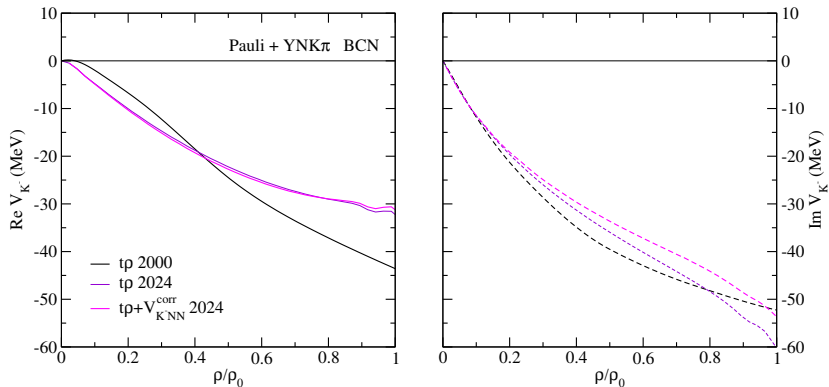


Figure: Real (left) and imaginary (right) parts of the total K^- potential calculated with Pauli + YNK π (magenta) BCN amplitudes for $E_{K^-} = m_{K^-}$ compared with K^- optical potential including kaon and π SE from Oset, Ramos, NPA 671 (2000) (black). Thin violet lines represent the $t\rho$ part of the current K^- optical potential obtained with Pauli YNK π BCN amplitudes.